Nanoscale Res Lett (2009) 4:1146–1152
DOI 10.1007/s11671-009-9373-z

NANO EXPRESS

Shell-Controlled Photoluminescence in CdSe/CNT Nanohybrids

Hua-Yan Si · Cai-Hong Liu · Hua Xu · Tian-Ming Wang · Hao-Li Zhang

Received: 9 May 2009 / Accepted: 3 June 2009 / Published online: 14 June 2009

Abstract A new type of nanohybrids containing carbon nanotubes (CNTs) and CdSe quantum dots (QDs) was prepared using an electrostatic self-assembly method. The CdSe QDs were capped by various mercaptocarboxylic acids, including thioglycolic acid (TGA), dihydrolipoic acid (DHLA) and mercaptoundecanoic acid (MUA), which provide shell thicknesses of ~5.2, 10.6 and 15.2 Å, respectively. The surface-modified CdSe QDs are then self-assembled onto aridine orange-modified CNTs via electrostatic interaction to give CdSe/CNT nanohybrids. The photoluminescence (PL) efficiencies of the obtained nanohybrids increase significantly with the increase of the shell thickness, which is attributed to a distance-dependent photo-induced charge-transfer mechanism. This work demonstrates a simple mean for fine tuning the PL properties of the CdSe/CNT nanohybrids and gains new insights to the photo-induced charge transfer in such nanostructures.

Keywords Carbon nanotubes · CdSe · Nanohybrids · Photoluminescence · Charge transfer

Introduction

Recently, nanohybrids containing both semiconductor quantum dots (QDs) and carbon nanotubes (CNTs) have been the subject of great interest as a consequence of the development of methods for the chemical modification of CNTs and the seeking for novel functional materials [1–4]. Attachment of QDs onto conducting CNTs would place a metallic wire in direct chemical contact with the QDs surface. The metallic CNTs could then promote direct charge transport and efficient charge transfer from the QDs [5–8]. This system has the potential to significantly increase the efficiency of photovoltaic devices [9, 10]. Besides, there has been an increasing interest on using CNTs in biological system [11]. Attaching QDs onto CNT can afford fluorescent labels and be utilized for detection, imaging and cell sorting in biological applications [12].

For all the above applications, the understanding to how the nanohybrid structure affects the charge transfer and energy transfer behaviors between the QDs and CNT is crucial. The interactions between II–VI QDs (such as CdS, CdSe and CdTe) and CNTs have been investigated by several groups [8, 13–15]. The charge-transfer efficiencies were evaluated by studying the changes in the photoluminescence (PL) [13, 16, 17] or photo-electrochemical properties of such hybrid materials [8, 14, 15, 18]. The PL behaviors of the nanohybrids were found to be strongly dependent on how the QDs are attached to the CNTs. For example, strong PL quenching by charge-transfer mechanism were reported for the CdS/TOAB/CNT [8], CdSe/pyridine/CNT [19] and CdSe/pyrene/CNT systems [20]. Partial emission quenching was observed on nanohybrids consisting of dendron-modified CdS QDs on CNT [21]. In contrast, Giersig [22, 23] reported preserved CdTe PL by insulating the CNTs using silica coating. The previous works have shown that the PL properties of the QD/CNT nanohybrids are strongly dependent on QD-CNT separation, but precise control to the distance between QDs and CNT was difficult to achieve in the available systems.

In this work, a facile strategy toward novel CdSe/CNT nanohybrids with tunable QDs-CNT separation is presented (Scheme 1). In this method, the CdSe QDs are

H.-Y. Si · C.-H. Liu · H. Xu · T.-M. Wang · H.-L. Zhang (✉)
State Key Laboratory of Applied Organic Chemistry, College of Chemistry and Chemical Engineering, Lanzhou University, 730000 Lanzhou, China
e-mail: Haoli.zhang@lzu.edu.cn

capped by different mercaptocarboxylic acids. The mercaptocarboxylic acids provide both necessary surface functionality and well-controlled shell thickness. The CNTs are noncovalently functionalized by positively aromatic molecules [24]. The CdSe QDs are then self-assembled onto the functionalized CNTs through electrostatic interaction to afford stable nanohybrids in aqueous solution. By using different mercaptocarboxylic acids, the average distance between QDs and CNTs in the CdSe/CNT nanohybrids can be readily adjusted within angstrom level precision. The obtained CdSe/CNT nanohybrids provide a well-defined system to study the effects of CdSe–CNT separation on their optical properties.

Experiment

Mercaptocarboxylic Acids Modified CdSe QDs

Trioctylphosphine oxide (TOPO)-capped CdSe QDs were prepared as reported previously [25]. The QDs were then modified by mercaptocarboxylic acids through a ligand-exchange reaction as described below. The thioglycolic acid (TGA) was diluted to 1 M with PBS (pH = 7.4) buffer. The TGA solution (3 mL) was added to the solution TOPO/CdSe, which was dissolved in 1 mL of chloroform. The mixture was stirred for 2 in dark and then separated into two layers spontaneously. The water layer was extracted and centrifuged to produce a pellet of TGA-capped QDs (TGA-CdSe). The supernatant, which contains free TGA, was discarded. Dihydrolipoic acid (DHLA)-capped CdSe QDs (DHLA-CdSe) were prepared as reported previously [26]. The mercaptoundecanoic acid (MUA)-capped CdSe QDs (MUA-CdSe) was prepared in a similar way as the TGA-CdSe, except that MUA was dissolved in ethanol. The mercaptocarboxylic acids modified CdSe QDs were purified by three cycles of filtration using membrane separation filters followed by washing with MilliQ ultra-pure water. Small amount of potassium tert-butoxide was added to the CdSe QDs solution to improve the solubility in water and also turn the QDs into a negatively charged state.

Aridine Orange-Modified CNT

Multiwall CNTs were purified in 37% HCl. The purified CNTs were then noncovalently modified with aridine orange (AO), following the processes described in our previous work [24]. The molecular structure of AO is shown in Scheme 1. In a typical process, 2.0 mg purified CNTs were added to an aqueous solution containing 2 mg AO and sonicated at room temperature for at least 2 h to reach a maximum adsorption. The AO-modified CNTs (AO/CNTs) were separated from the solution by filtration using a 0.22-μm diameter cellulose acetate–cellulose nitrate membrane, and then thoroughly rinsed to remove access AO.

CdSe/CNT Nanohybrids

The aqueous solutions of CdSe QDs were then titrated with AO/CNT solution and gently stirred to give the CdSe/CNT nanohybrids. The produced nanohybrids were subjected to three washing cycles to remove the excess CdSe QDs. In each washing cycle, the samples were centrifuged at 4,000 rpm for 3 min then redispersed in PBS buffer after removing the supernatant.

Results and Discussions

The CNTs were first modified by AO molecules via π–π stacking. The interaction between CNTs and different organic dyes has been investigated in our previous

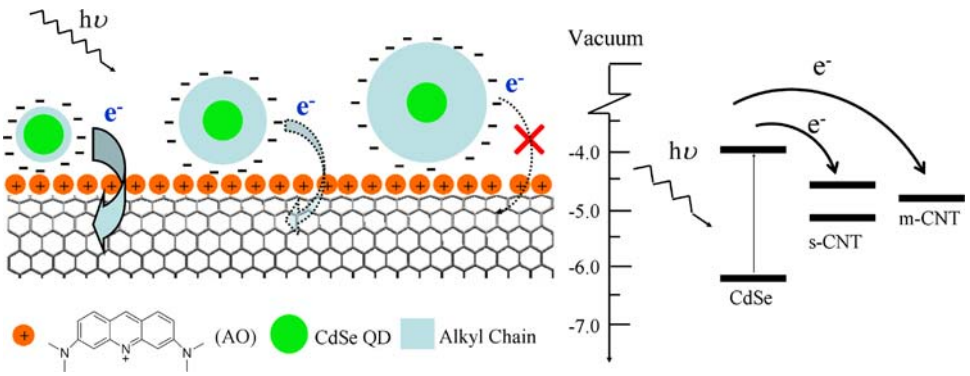

Scheme 1 Schematic illustration to the structures of the CdSe/CNT nanohybrids prepared by electrostatic assembly (*left*). The photo-induced charge-transfer efficiency within the nanohybrids is controlled by the shell thickness. Energy-level diagram and possible charge-transfer process for the conjugate complex between CdSe QDs and semiconducting CNTs (s-CNT) or metallic CNTs (m-CNT) are illustrated in the *right*

work [24]. Positively charged AO shows high affinity to CNTs and strongly improved the dispersibility of CNTs in aqueous solution. After being functionalized by AO, the CNTs can be readily dispersed in aqueous medium to form stable suspensions. Figure 1a and b shows the typical TEM images of CNTs before and after the modification by AO. Figure 1b suggests that most of the AO functionalized nanotubes are in less entangled state than the unmodified CNTs. The topographies of the CNTs after interaction with different CdSe QDs are shown in Fig. 1c–e. The TEM micrographs indicate that QDs and the modified CNTs coexist in the proximity of each other. The increased entanglement of the nanotubes compared with that of AO/CNTs (Fig. 1b) could be attributed to the strong electrostatic interactions between the negatively charged quantum dots and the AO functionalized CNTs. The coverage of the QDs on the CNTs appears to be not very uniform, suggesting that the positive charge on the CNT surface is not very uniform. This nonuniformity may be attributed to the defects on the CNTs. The CNT samples were purified in acid before AO modification, and therefore contain many –CHO, –OH and –COOH groups (as shown in the IR data below). These groups, especially –COOH, may interact with the AO molecules and partially neutralize the positive charges and induce a nonuniformed distribution of surface charge.

The bonding between the mercaptocarboxylic acid-capped CdSe QDs, and the AO/CNTs was first studied by comparing their XRD patterns (Fig. 2). The AO/CNT sample produces two typical peaks at 26.06° and 44.46°, which are attributed to the (002) and (100) planes of CNTs [27] (Fig. 2a). The CdSe/CNT composite gives broad peaks at 22°, 25.6°, 26.8°, 42° and 49.6°, attributed to the (100), (002), (101), (102) and (112) planes of the hexagonal phase CdSe (close to PCPDFWIN 77-2307), respectively. The (100), (002) and (101) peaks of the CdSe QDs are partly overlapped with the (002) peak of the oxidized CNTs, therefore are difficult to be identified (Fig. 2b). No peak corresponding to impurities is detected. The CdSe peaks in the XRD patterns of the CdSe/CNT nanohybrids

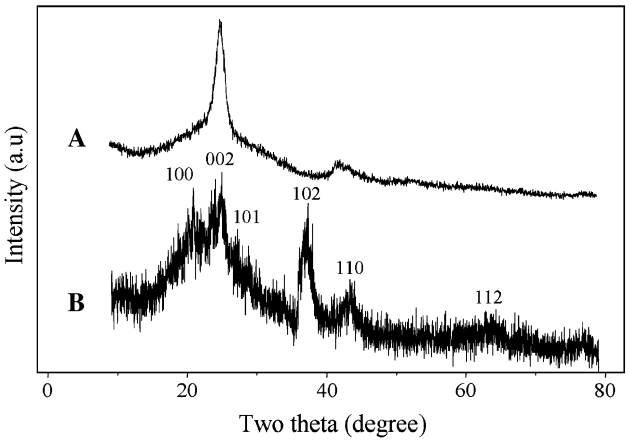

Fig. 2 XRD patterns of **a** AO/CNTs and **b** TGA-CdSe/CNT nanohybrids

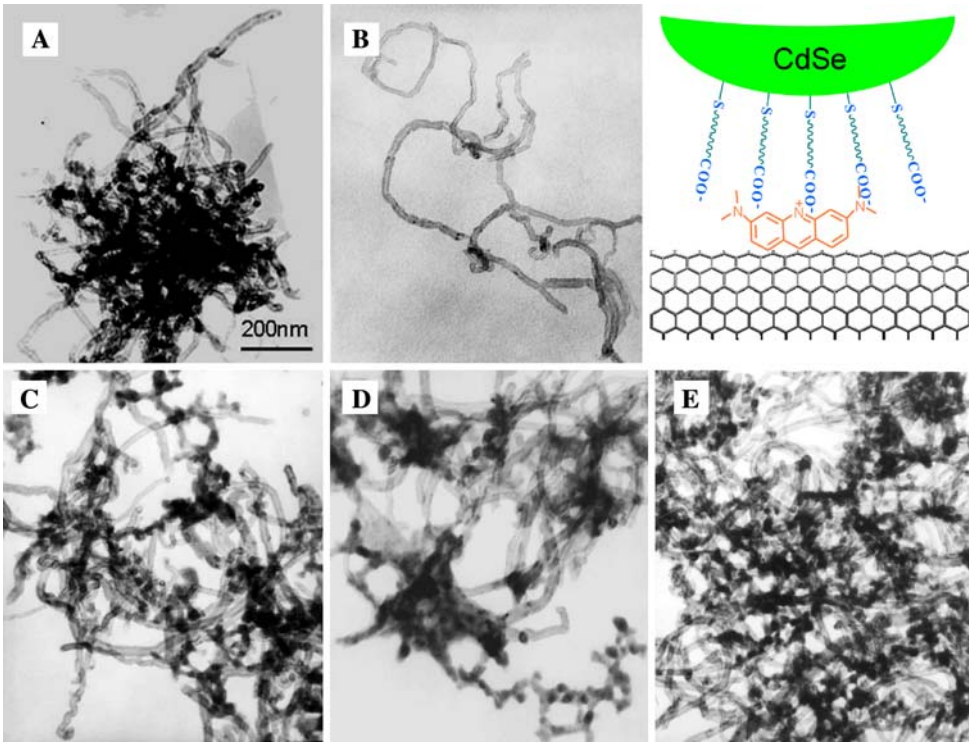

Fig. 1 TEM micrographs of **a** The purified CNTs, **b** AO/CNTs, **c** TGA-CdSe/CNT, **d** DHLA-CdSe/CNT and **e** MUA-CdSe/CNT

are all very broad (Fig. 2b), which is attributed to the small size of the CdSe QDs. The XRD data are in support of the successful attachment of the hexagonal phase of CdSe QDs to the surface of CNTs. Similar observations were found for the DHLA-CdSe/CNT and MUA-CdSe/CNT nanohybrids.

FT-IR spectra also confirm the formation of CdSe/CNT nanohybrids. Due to the surface oxidation, the acid-treated CNTs show characteristic peak of C=O stretching at 1,630, corresponding to oxidized spices, such like –COOH and –CHO (Fig. 3a). The presence of AO on the AO/CNTs is evident by a series of absorption bands in the regions of 1,000–1,500 cm^{-1}, which are consistent with the characteristic peaks of AO in this region (Fig. 3b). The TOPO/CdSe shows a strong band around 1,100 cm^{-1} due to the P=O stretch of the TOPO ligand [28] (Fig. 3c). Evidence of that the QDs are capped with TGA comes from the presence of a strong –COOH peak at 1,680 cm^{-1} and vanish of the P=O stretch band around 1,100 cm^{-1} (Fig. 3d), indicating that the desired ligand exchange occurred on the QD surface. Assembly of TGA-CdSe QDs onto the AO/CNTs results in the appearance of a new peak at 1,730 cm^{-1}, and the vibrational mode at 1,580 cm^{-1} on the TGA-CdSe nanoparticles shifts to 1,550 cm^{-1} (Fig. 3e), revealing the interactions between the carboxylate group on TGA-CdSe and the pyridine ring of the AO molecules on the CNTs. The interaction between the CNTs and the QDs can be ascribed to the electrostatic interaction between the positively charged AO moieties and the carboxylate groups [29]. Because the AO molecule has a pK_b of 7.2, the AO/CNTs should show positive surface charge under slightly acidic conditions. The mercaptocarboxylic acid on the CdSe QDs could afford negatively charged carboxylate groups, hence could associated with the AO moieties on the CNTs to yield CdSe/CNT nanohybrids. Even when both are initially in the neutral state, acid–base reaction could

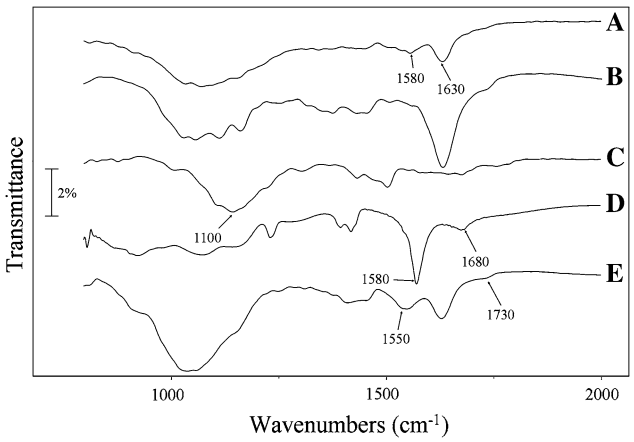

Fig. 3 FT-IR spectra of **a** Acid-purified CNTs, **b** AO/CNTs, **c** TOPO-CdSe QDs, **d** TGA-CdSe QDs and **e** TGA-CdSe/CNT nanohybrids

take place between the AO and surface-bound acids. Similar observations were also found for the DHLA-CdSe/CNT and MUA-CdSe/CNTs nanohybrids.

To probe the interaction between QDs and CNTs, we titrated the aqueous solutions of DHLA-CdSe with the AO/CNT solution and monitored the changes in the characteristic band gap transitions of CdSe in both absorption and PL spectra. In the absorption spectra, the features of CNT unequivocally emerge during the titration. A consistent trend in all of these titration curves is a shift of the CdSe absorption edge around 580 nm toward higher transition energies reaching a few nanometers. In the PL spectra, the addition of CNT solutions leads to nonlinear quenching effects of the strong CdSe-centered emission around 560 nm (Fig. 4). Strong electronic interactions, such as transfer of charge density between the electroactive components, are likely to be responsible for the aforementioned effects, i.e., the blue shift in absorption edge and PL quenching.

The changes in the CdSe/CNT absorption and the PL spectra can be understood by the photo-induced charge transfer within the nanohybrids (Scheme 1). The valence band and conduction band energy levels for the as-prepared CdSe QDs are taken to be 6.2 and 3.9 eV, respectively [30]. The semiconducting CNTs normally have an energy gap ranging from 0 to 1.1 eV, and the Fermi level of the metallic CNTs is taken to be 4.5–5.0 eV [31, 32]. The PL of the QDs is due to the radiative decay path from their excited state to ground state [14]. Given that the nanotubes quenched the CdSe QDs, the QD-CNT interaction must provides an alternative nonradiative decay path. It is believed that this nonradiative decay path occurs because the difference in electron affinity between the CdSe QDs and the CNTs is sufficient to allow electron transfer from the QDs to the CNTs [19]. Based on the energy diagram, the formation of CdSe/CNT conjugates favors the electron transfer from the QDs (donor) to the CNTs (acceptor) such that the excited electrons moved to the CNTs rather than be emitted as the PL peak. Thus, the electrons of the excitons could be partially transferred to CNTs by an electron-injection mechanism, while the remaining electrons exhibit a reduced emission by an electron-hole recombination process.

As the titration experiment shows that the amount of the added CNTs strongly affects the absorption and PL properties of the CdSe QDs, the spectra of the three CdSe/CNT nanohybrids were measured in the presence of little excess CNTs. Figure 5 shows the UV–vis absorption and PL spectra of the aqueous suspensions of the different CdSe QDs and the CdSe/CNT nanohybrids. Figure 5a shows the characteristic exciton absorption peaks at 550, 540, 560 nm for the TGA-CdSe, DHLA-CdSe and MUA-CdSe QDs, respectively, which are corresponding to their first

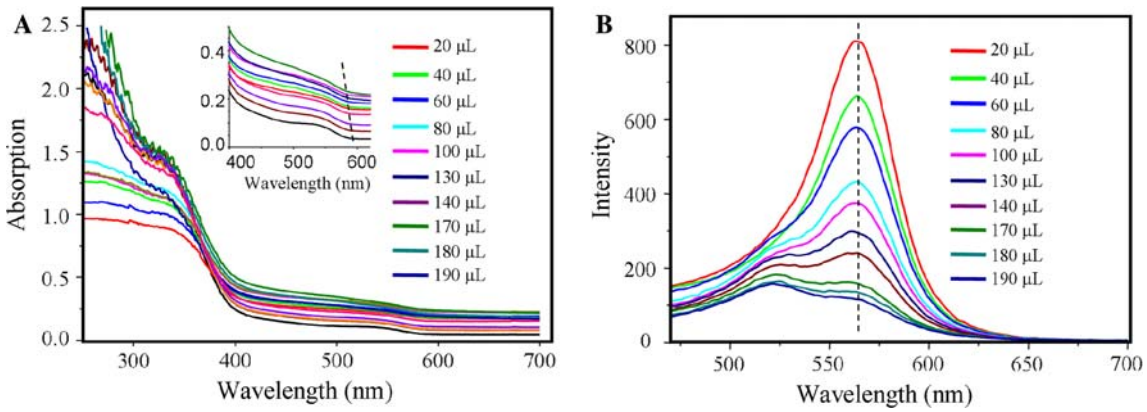

Fig. 4 The UV–vis absorption (**a**) and photoluminescence spectra (under excitation at 400 nm) (**b**) of CdSe QDs upon addition of AO/CNTs. The insert of (**a**) shows the slight blue shift of the CdSe absorption edge during titration

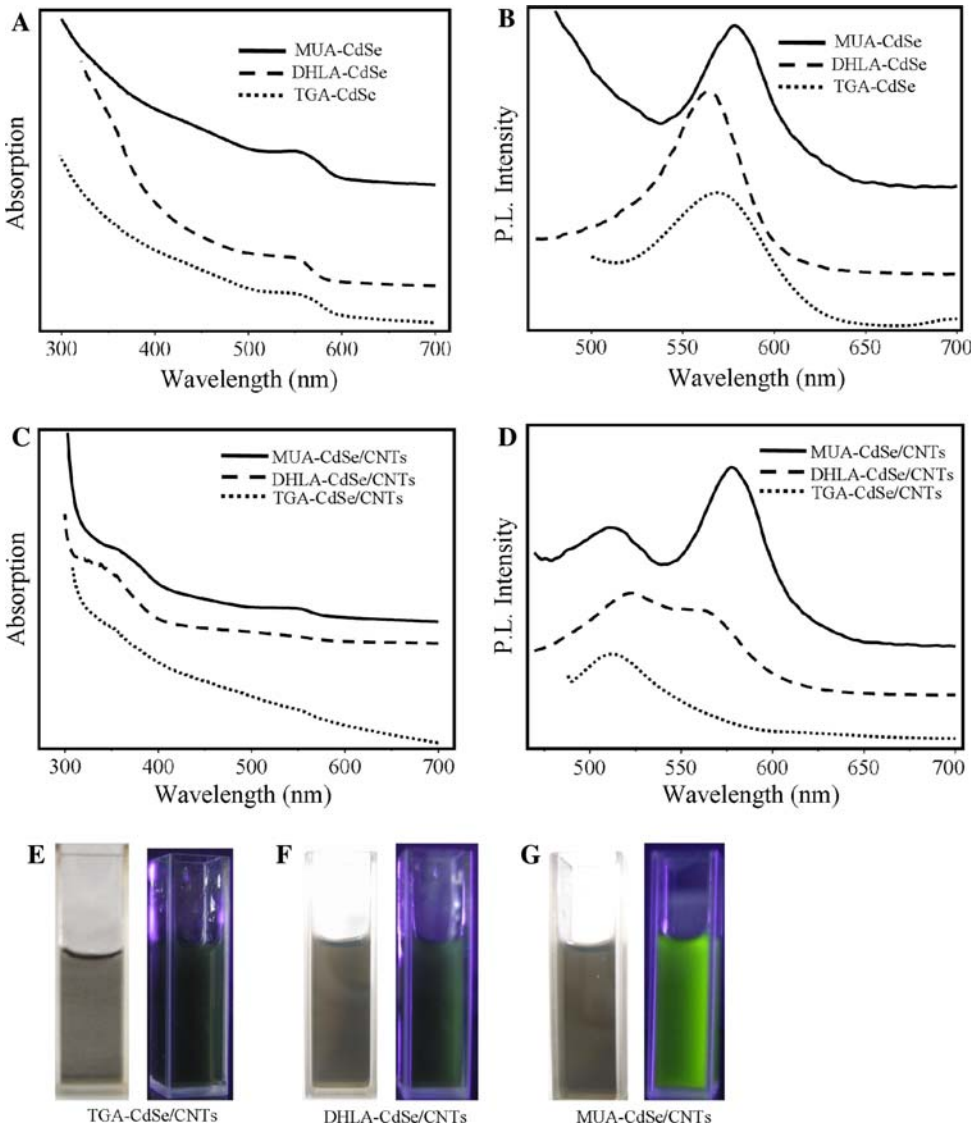

Fig. 5 **a** UV–vis absorption and **b** photoluminescence spectra of aqueous CdSe QDs. **c** UV–vis absorption and **d** photoluminescence spectra of the CdSe/CNT nanohybrids. **e–g** Are the optical and photoluminescence images (365 nm irradiation) of the nanohybrids suspensions. The *curves* are offset for clarity

electronic transition. The small variation in the exciton peak positions in the three QDs is attributed to the small difference in the average particle sizes. This size variation is relatively small and should not affect our further discussions. The TGA-CdSe, DHLA-CdSe and MUA-CdSe QDs show strong PL peaks at 570, 560 and 580 nm, respectively (Fig. 5b). The PL spectra of the CdSe/CNT nanohybrids reveal an additional luminescence feature at 520 nm, corresponding to the emission from the AO molecules (Fig. 5d). The existence of this characteristic AO peak confirms the presence of AO on the CNT sidewalls [24]. After forming the CdSe/CNT hybrid, the absorption peaks of the QDs are slightly blue-shifted and broadened (Fig. 5c). The intensity of the QD peaks were also reduced compared to that in free states. In previous studies on the CdTe and CdSe QDs that were covalently attached to CNTs [1, 33], no QD absorption band was observed due to the broad background absorption of the CNTs. In our work, although the CNT background seems to be strongly screening the absorption of the QDs, the QD absorption edge around 550–580 nm can still be distinguished (Fig. 5c), which can only be explained by a dense coating of relatively monodisperse QDs onto the CNTs [23].

As mentioned above, the different mercaptocarboxylic acid coatings provide different shell thicknesses for the CdSe QDs. The PL spectra show that the intensity of the QD emission peaks in the CdSe/CNT nanohybrids is strongly dominated by the shell thickness. The PL of the TGA-CdSe QDs is nearly completely vanished after binding with the CNTs. The PL of the DHLA-CdSe QDs is dramatically reduced to a moderate intensity, indicating partial quenching occurred. In contrast, the PL intensity of the MUA-CdSe QDs remains nearly unchanged in the presence of the CNTs (Fig. 5d) and showing no obvious quenching occurs. The different PL intensities of the CdSe/CNT nanohybrids suspensions are visible to naked eyes in the fluorescent images of the nanohybrid solution. As seen in Fig. 5e–g, under UV irradiation, the PL brightness increases with the chain length of the capping mercaptocarboxylic acids on the CdSe QDs.

As demonstrated in Fig. 5, the fluorescence of the CdSe/CNT is well controlled by the length of the organic spacers. In a similar fashion, Kulakowich et al. [34] studied the optical effects of tuning the separation between gold colloids and QDs on planar substrates. A clear increase of the PL has been observed as the separation increased. In our strategy, the separation between the QDs and CNTs is adjusted by the lengths of alkyl chains of the capping agents. The fully extended lengths of TGA, DHLA and MUA are 5.2, 10.6 and 15.2 Å, respectively, as estimated from semi-empirical (PM3) calculations. Assuming that the AO molecules are adsorbed on the CNT sidewalls with a coplanar configuration and using the normal van der Waals diameter values for the AO and carboxylic acids, the separation between the edges of the CdSe QDs and CNTs are estimated to be around 14, 19 and 24 Å for the TGA-CdSe/CNT, DHLA-CdSe/CNT and MUA-CdSe/CNT systems, respectively. As the average distance between the CdSe QDs and CNTs increases within 10 Å ranges, the PL properties of the CdSe/CNT change from total quenching to nearly no quenching. This result clearly demonstrates that a precise control to the QD-CNT spacing at angstrom level is essential for controlling the PL properties of the CdSe/CNT nanohybrids.

Conclusions

We report a new and facile method for attaching CdSe QDs onto CNT surface by electrostatic self-assembly. By using different mercaptocarboxylic ligands, the shell thicknesses of the CdSe QDs are well controlled within angstrom-level precision. The formation of various CdSe/CNT nanohybrids has been confirmed by TEM, XRD, FT-IR, UV–vis absorption and PL spectroscopies. The absorption and PL spectra of the hybrid materials suggested that photo-induced electron transfer from CdSe QDs to CNTs took place in the nanohybrids. The efficiency of the PL quenching decreases upon increasing the shell thickness due to the distance-dependent electron transfer efficiency. This work demonstrates that the shell thickness control to the QDs opens up a straightforward methodology for investigating the interaction between fluorescent nanomaterials coupled with CNTs. Since there is large number of bifunctional ligands readily available for researchers, this method can be used as a general approach to tailor the QD-CNT separation within molecular size range. The ability to allow or prevent charge transfer from photoexcited QDs to CNT provides a useful technique in developing QDs/CNT nanomaterials to become flexible, facile building blocks for many practical applications, including electrooptic devices, biological nanoprobes for cytological investigation and in situ fluorescently detectable microsensors.

Acknowledgments The authors are grateful to the financial support from the program for New Century Excellent Talents in University (NCET), National Natural Science Foundation of China (NSFC. 20503011, 20621091), Specialized Research Fund for the Doctoral Program of Higher Education (SRFDP. 20050730007), and Key Project for Science and Technology of the Ministry of Education of China (106152).

References

1. J.M. Haremza, M.A. Hahn, T.D. Krauss, Nano Lett. **2**, 1253 (2002)

2. S. Banerjee, S.S. Wong, Nano Lett. **2**, 195 (2002)
3. S. Agrawal, A. Kumar, M.J. Frederick, G. Ramanath, Small **1**, 823 (2005)
4. B.R. Azamian, K.S. Coleman, J.J. Davis, N. Hanson, M.L.H. Green, Chem. Commun. **4**, 366 (2002)
5. B.J. Landi, S.L. Castro, H.J. Ruf, C.M. Evans, S.G. Bailey, R.P. Raffaelle, Sol. Energy Mater. Sol. Cells **87**, 733 (2005)
6. G.M.A. Rahman, D.M. Guldi, E. Zambon, L. Pasquato, N. Tagmatarchis, M. Prato, Small **1**, 527 (2005)
7. S. Ravindran, S. Chaudhary, B. Colburn, M. Ozkan, C.S. Ozkan, Nano Lett. **3**, 447 (2003)
8. I. Robel, B.A. Bunker, P.V. Kamat, Adv. Mater. **17**, 2458 (2005)
9. D.M. Guldi, I. Zilbermann, G. Anderson, N.A. Kotov, N. Tagmatarchis, M. Prato, J. Mater. Chem. **15**, 114 (2005)
10. P.V. Kamat, J. Phys. Chem. C **111**, 2834 (2007)
11. N.N. Ratchford, S. Bangsaruntip, X.M. Sun, K. Welsher, H.J. Dai, J. Am. Chem. Soc. **129**, 2448 (2007)
12. S. Chaudhary, J.H. Kim, K.V. Singh, M. Ozkan, Nano Lett. **4**, 2415 (2004)
13. W. Li, C. Gao, H. Qian, J. Ren, D. Yan, J. Mater. Chem. **16**, 1852 (2006)
14. D.M. Guldi, G.M.A. Rahman, V. Sgobba, N.A. Kotov, D. Bonifazi, M. Prato, J. Am. Chem. Soc. **128**, 2315 (2006)
15. L. Sheeney-Haj-Ichia, B. Basnar, I. Willner, Angew. Chem. Int. Ed. **44**, 78 (2005)
16. V. Biju, T. Itoh, Y. Baba, M. Ishikawa, J. Phys. Chem. B **110**, 26068 (2006)
17. B.F. Pan, D.X. Cui, C.S. Ozkan, M. Ozkan, P. Xu, T. Huang, F.T. Liu, H. Chen, Q. Li, R. He, F. Gao, J. Phys. Chem. C **112**, 939 (2008)
18. J.M. Du, L. Fu, Z.M. Liu, B.X. Han, Z.H. Li, Y.Q. Liu, Z.Y. Sun, D.B. Zhu, J. Phys. Chem. B **109**, 12772 (2005)
19. Q.W. Li, B.Q. Sun, I.A. Kinloch, D. Zhi, H. Sirringhaus, A.H. Windle, Chem. Mater. **18**, 164 (2006)
20. L.B. Hu, Y.L. Zhao, K.M. Ryu, C.W. Zhou, J.F. Stoddart, G. Grüner, Adv. Mater. **20**, 939 (2008)
21. S.H. Hwang, C.N. Moorefield, P.S. Wang, K.U. Jeong, S.Z.D. Cheng, K.K. Kotta, G.R. Newkome, J. Am. Chem. Soc. **128**, 7505 (2006)
22. M. Olek, T. Busgen, M. Hilgendorff, M. Giersig, J. Phys. Chem. B **110**, 12901 (2006)
23. M. Grzelcaak, M.A. Correa-Duarte, V. Salgueirino-Maceira, M. Giersig, R. Diaz, L.M. Liz-Marzan, Adv. Mater. **18**, 415 (2006)
24. C.H. Liu, J.J. Li, H.L. Zhang, B.R. Li, Y. Guo, Colloids Surf. A Physicochem. Eng. Asp. **313–314**, 9 (2008)
25. H.Y. Si, Z.H. Sun, H.L. Zhang, Colloids Surf. A Physicochem. Eng. Asp. **313–314**, 604 (2008)
26. H.T. Uyeda, I.L. Medintz, J.K. Jaiswal, S.M. Simon, H. Mattoussi, J. Am. Chem. Soc. **127**, 3870 (2005)
27. M. Terrones, W.K. Hsu, A. Schilder, H. Terrones, N. Grobert, J.P. Hare, Y.Q. Zhu, M. Schwoerer, K. Prassides, H.W. Kroto, D.R.M. Walton, Appl. Phys. A **66**, 307 (1998)
28. M.J. Eilon, T. Mokari, U.J. Banin, J. Phys. Chem. B **105**, 12726 (2001)
29. Z.X. Cai, X.P. Yan, Nanotechnology **17**, 4212 (2006)
30. M. Gratzel, Nature **414**, 338 (2001)
31. S. Kazaoui, N. Minami, N. Matsuda, Appl. Phys. Lett. **78**, 3433 (2001)
32. M. Shiraishi, M. Ata, Carbon **39**, 1913 (2001)
33. S. Barnerjee, S.S. Wong, Adv. Mater. **16**, 34 (2004)
34. O. Kulakowich, N. Strekal, A. Yaroshevich, S. Maskevich, S. Gaponenko, I. Nabiev, U. Woggon, M. Artemyev, Nano Lett. **2**, 1449 (2002)